33RD CONGRESS
OF THE INTERNATIONAL COUNCIL
OF THE AERONAUTICAL SCIENCES
STOCKHOLM, SWEDEN, 4-9 SEPTEMBER, 2022

ICAS 2022 SWEDEN

FLIGHT DYNAMICS SIMULATION AND FCS AUTO-GENERATION IN THE CONCEPTUAL DESIGN PHASE OF AN UNSTABLE SUPERSONIC AIRCRAFT

Emil Johansson[1], Philip Månsson[1] & Patrik Sjöberg[1]

[1]Saab Aeronautics, Linköping, Sweden

Abstract

The assessement of the achievable manoeuvrability of an aircraft concept is often limited to simple handbook methods during the conceptual design phase. These methods are not necessarily well suited for a highly manoeuvreable fly-by-wire aircraft design. More comprehensive early design feedback is possible by using a 6-DoF flight mechanics model with automatically generated control laws. The described method also allows for faster design iterations. A parametrisation of key design features facilitates an improved exploration of design trades. The method is exemplified with a simulation model and control laws developed within the Saab Future Combat Aircraft System (Saab FCAS) project. The usage of the flight mechanics model has increased the efficiency of the conceptual design and aided the sizing of various subsystems of the aircraft.

Keywords: flight dynamics simulation, control laws, aircraft conceptual design, dynamic inversion, control allocation

1. Introduction

This paper describes the usage of a flexible flight mechanics simulation model with automatically generated control laws in the conceptual development phase of an unmanned supersonic aircraft. The principle of the model and the control law design is explained, together with examples of how the model can be used to provide early design feedback.

During the concept development phase of a new aircraft, the design team is often bound to simple handbook methods when it comes to assessing the achievable manoeuvrability and the desired stability of the aircraft. Methods that provide faster and more comprehensive insights are necessary in order to reduce the traditionally long development lead times and to handle the increased complexity in aircraft development projects. It is of particular interest to increase the knowledge and the design freedom earlier in the design process of more unconventional aircraft configurations, for which the handbook methods are less reliable[1].

Classical handbook methods regarding FQ/HQ are often limited to studying the longitudinal and lateral/directional degrees of freedom separately. For a highly manoeuverable aircraft, the coupled dynamic response is often a limiting factor. Being able to analyse the coupled reponse early on in the design process is a strong tool to acheive a good overall manoeuvering capability. This can be achieved by incorporating a flight control system (FCS) in the simulation model to be used in the conceptual design loop. It is also possible to obtain more comprehensive insights into the mission capability of a conceptual design. Another result is the broadening of integrated aspects for various subsystems. This leads to a more optimal design where additional subsystems are designed with respect to the flight mechanics capability.

The simulation model with control laws is developed within the Saab Future Combat Aircraft System (Saab FCAS) project. Manned and unmanned aircraft are studied as part of the project. The challenges of designing these types of aircraft have created the need and initiated the development of the methodology described in this paper. In particular, a concept for an unmanned supersonic aircraft has been used as a platform in the development of this methodology, see Figure 1.

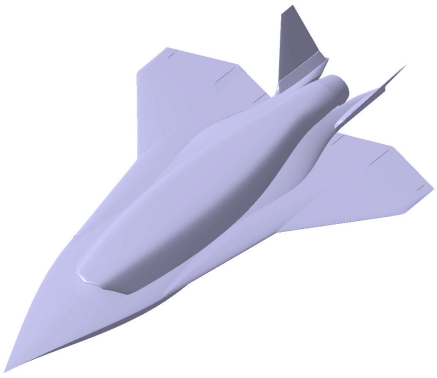

Figure 1 – Saab FCAS unmanned concept aircraft

2. Simulation Model

With a baseline conceptual design of the aircraft it is possible to create an aerodynamic data set using CFD software. Together with basic inertia data from the CAD model and a preliminary engine model for the engine thrust it is possible to create a complete aircraft model useful for dynamic simulations. The model can then be used to evaluate mission requirements as illustrated in Figure 2.

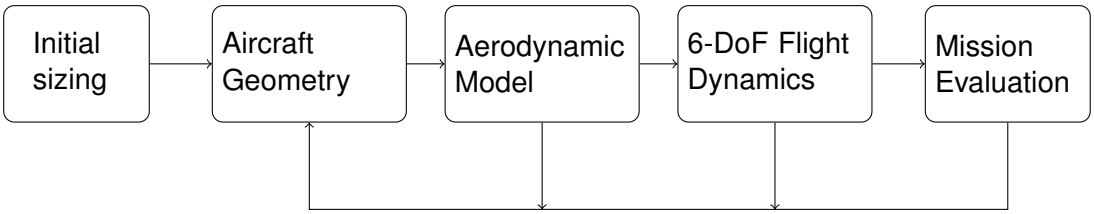

Figure 2 – Flight dynamics in the conceptual design loop

It is desirable to be able to keep key design parameters flexible for as long as possible in the design process to find the best overall design for the mission requirements. In order to reduce the number of full design iterations where CAD modelling and analysis with CFD is necessary, the flight dynamics solver incorporates models for several design parameters. In this case, many of the aircraft properties are parametrised such that design changes can be applied at the simulation level in runtime. Examples of these properties are:

- Centre of gravity positon
- Moments of inertia
- Available control power
- Control surface deflection rate
- Landing gear arrangement
- Manoeuvre authority

Control power, also denoted as control authority, refers to the aerodynamic moment about the Centre of Gravity (CG) which can be generated by the control surfaces. The manoeuvre authority refers to the model reference parameters including the manoeuvre and responsiveness targets. Examples of those parameters are effective time delays for changes in commanded angular rate and limits for the maximum allowed roll rate and load factor. By varying the parameters in the simulation model, it is possible to find desired target values that can be used in the next full design iteration that provides an updated aerodynamic dataset to the flight mechanics model.

2.1 Control Surface Modelling

The control power is varied by using a model that generates scaling factors which are used to scale the associated aerodynamic coefficients. This can be done either explicitly or through geometric definition, by which it is possible to scale, add/remove and position the control surfaces. In order to approximate and simulate different control surface geometries, the scaling model is constrained by the outline of the planform. Thus, the resized control surfaces will not affect the basic stability of the aircraft and require an update of the aerodynamic data with additional CFD simulations.

The FCS accounts for the reconfigured control power and the number of control surfaces within the simulation environment. The control laws are configured to provide control allocations for best overall performance. Figure 3 shows an example of a use case of the flexibility of the model. The baseline two elevon(blue) design is updated to three elevons(green) of increased elevon-to-wing chord ratio, c_e/c_w. The aerodynamic coefficents are updated for each control surface(not shown). The model updates the aerodynamic coefficients based on effects such as area, moment arms, elevon leading edge angle, chord ratio and number of surfaces. As the design iterations proceed, the scaled aerodynamics are updated with more representative modelling of the new adaptations of the baseline. Areas are identified in which to improve the aerodynamic data set for increased accuracy in the analysis.

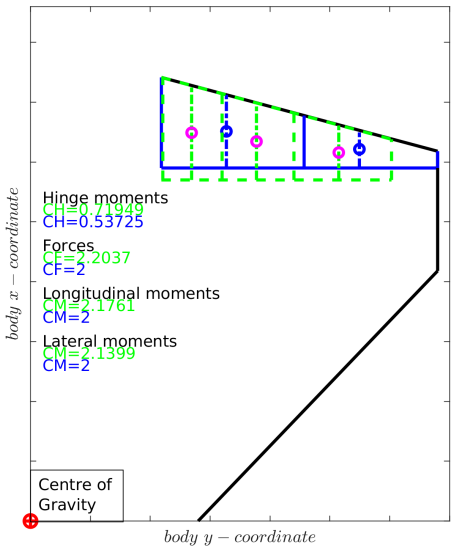

Figure 3 – Example of output from the control surface scaling model. Baseline - two elevons(blue), Resized- three elevons(green) .

3. Flight Control Laws

The flight mechanics simulation utilises a flight control system, which enables close to the maximum achievable manoeuvring capability given chosen parameter values. Many cost/benefit trade-offs can be shown when the maximum flight mechanics performance of a concept with varying parameters is

realised in a simulator. Flight control laws representative of a final design, which incorporate various configurable parameters, allow modelling of flight mechanics performance close to what is achievable for the concept. This is important in order to study the various trade-offs accurately.

In the conceptual design phase it is beneficial to be able to quickly construct control laws representative of a production level design. This is desired in order to facilitate faster iterations with varying aircraft models as shown in Figure 2. Faster iterations allow for more iterations or more concept developement in a given time frame.

In addition to being quick to generate with representative performance, the control laws facilitates an evaluation of

- The control power and actuation rate necessary to perform prescribed manoeuvres with varying rapidness.
- The maximum manoeuvre capability of a nominal aircraft configuration subject to variations in CG, control surface size, etc.

Quick evaluation possibilities are provided by allowing for variations in the simulation model during runtime. Figure 4 shows user inputs handled by the flight control laws when running the simulation model. The available inputs are grouped in manoeuvre demand inputs, reponse parameter inputs, and aircraft sizing parameters.

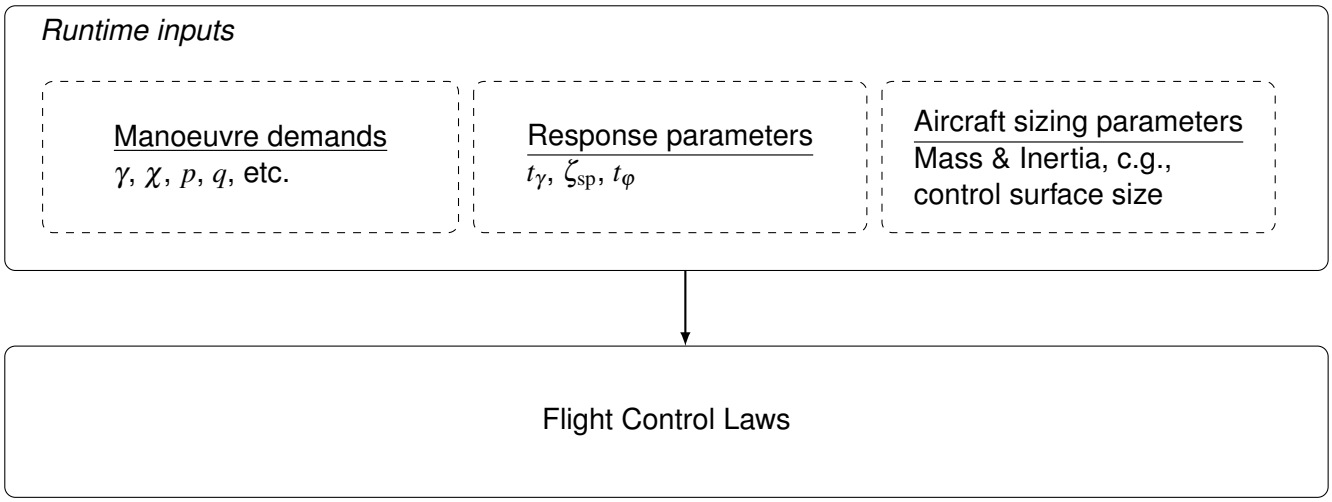

Figure 4 – Control law runtime inputs grouped into categories related to manoeuvre demands, response characteristics, and aircraft sizing variations.

Manoeuver demands can be low level commands such as aircraft pitch rate and roll rate. It is also possible to specify higher level demands, such as a desired fligth path (γ, χ) or flight trajectory, which are then converted to pitch, roll and yaw rate by an outer control loop.

The responsiveness of the aircraft to the manoeuver demands can be altered in order to evaluate the cost and benefit in terms of aircraft sizing and mission performance. The responsiveness parameters prescribe the equivalent of handling quality parameters for manned aircraft. Effective time delay for a flight path change, t_γ, short period damping ζ_{sp}, and effective time delay for a roll angle change, t_φ, are examples of possible parameters. The required responsiveness of an unmanned aircraft might be different compared with a manned fighter and that could in turn potentially alter the required control surface sizing.

It is also possible to change key aircraft sizing parameters in runtime in order to quickly evaluate its effects. A change in, for example, centre of gravity can then be propagated to representative changes in actuation requirements and thus, exposing this trade-off to an aircraft overall design level. Alternatively, the simulation environment can be used to facilitate an evaluation of the manoeuver capability with a set of sizing parameters. It is necessary to consider the uncertainty of aircraft sizing parameters such as mass and inertia in the conceptual design phase. It is therefore valuable to be able to evaluate and quantify the sensitivity of the performance of a more mature design due to these uncertainties.

3.1 Control Law Architecture

A goal of the control law is to explicitly track prescribed manoeuvers and to, for example, allow for varied control effectiveness. This maps well to the dynamic inversion formulation. Figure 5 shows a generalised overview of the flight control law which determines commanded control surface positions based on desired manoeuvres and measurements of the aircraft state.

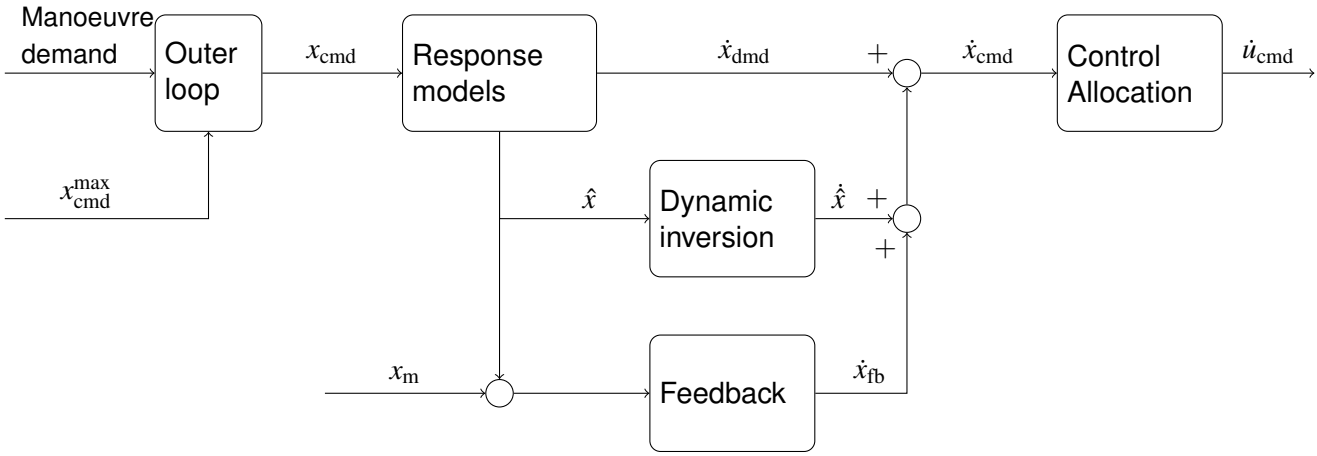

Figure 5 – Generalized control structure showing the signal flow from manoeuvre commands to control surface deflection commands.

The control law is made up of outer control loops which translates various manoeuvre demands to aircraft axis rotations in pitch, roll, and yaw, here denoted as $x_{\mathrm{cmd}} = [p_{\mathrm{cmd}}, q_{\mathrm{cmd}}, r_{\mathrm{cmd}}]$. The demanded rotation rates are going through response models and translated to demanded body-axis angular rate derivates, $\dot{x}_{\mathrm{dmd}} = [\dot{p}_{\mathrm{dmd}}, \dot{q}_{\mathrm{dmd}}, \dot{r}_{\mathrm{dmd}}]$ and expected aircraft state, $\hat{x}$. The response modelse changes with changes in the various response parameters.

The expected aircraft state $\hat{x}$ is fed into a model of the forces and moments acting on the aircraft, $\hat{\dot{x}}$, which is supposed to be canceled by moments from control surfaces. This is the dynamic inversion part of the control law. A feedback term, $\dot{x}_{\mathrm{fb}}$ which feeds back demanded aircraft rotations as a function of the difference between the expected aircraft state and the measured aircraft state, x_m is necessary for robustness, disturbance attenuation, and stabilisation of unstable modes.

The demanded moments from control surfaces are summed into $\dot{x}$ and allocated to the various control surfaces in the control allocation block. The control allocation block requires a linearization of the control effectiveness. Both the dynamic inversion and control allocation functions are adjusted if aircraft aerodynamic data or inertia are changed.

An explicit model following architecture for the control laws is chosen for multiple reasons. The evaluation of a closed-loop manoeuvre is aided by the possiblity of comparing actual aircraft motion with the prescribed motion. An undesireable response can then be identified as an issue related to either

a poorly chosen response model, or a deficient control loop where the prescribed response is not achieved.

The purpose of the outer loop control laws is to translate desired aircraft flight path and trajectories to commanded body axis rotations which is limited to $x_{\text{cmd}}^{\max}$. By being cognisant of the aircraft manoeuvre capability, the outer loops can be constructed such that maximum aircraft performance is utilised while still being independent of the aircraft model used.

3.2 Online Calculation of Available Manoeuvre Capability

To the extent that the manoeuvre capability is constrained by aircraft sizing parameters, variations in aforementioned parameters should result in changes of the attainable manoeuvre capability. An online calculation of the available manoeuvre limits given specified maximum control surface deflections is a solution to the problem of utilising close to the maximum manoeuvre capability with variations in aircraft parameters.

Figure 6 shows an overview of how the maximum allowed manoeuvre command is determined. The maximum allowed steady state manoeuvre is determined based on the allowed steady state control surface deflections and the current flight condition. Note that a steady state manoeuvre in this context is a combination of constant body axis rotation rates. This maximum is compared with other manoeuvre constraints such as angle of attack limits or structural limits on load factor and roll rate. The most limiting values are transformed to limitations on maximum steady state pitch rate and coordinated roll rate and denoted as $x_{\text{cmd}}^{\max}$.

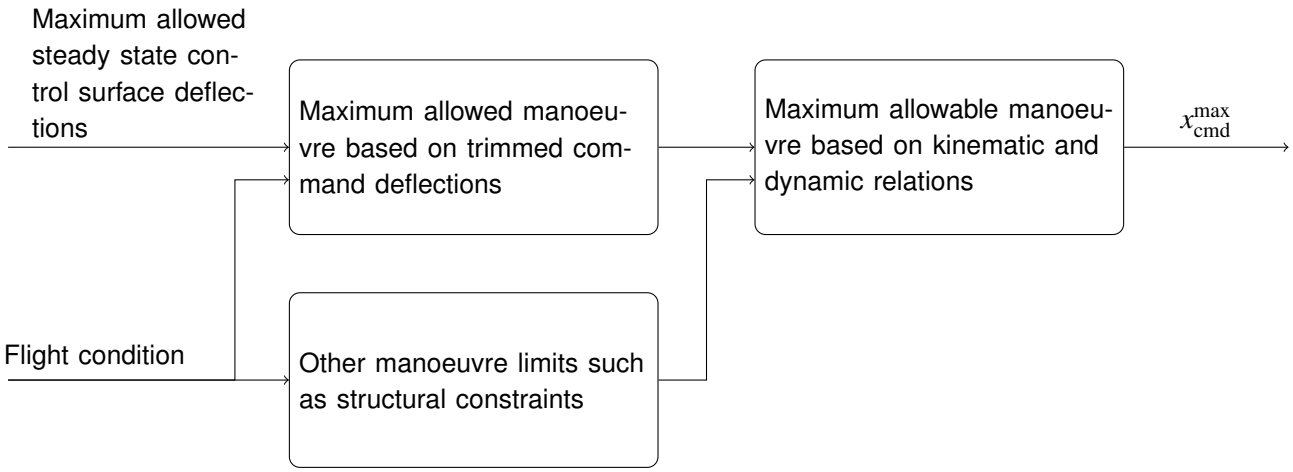

Figure 6 – Structure for determining maximum commandable angular rate at particular flight condition given constraints on steady state control surface deflections and other states.

4. Simulation Results

This section presents some highlights of the analyses used to determine the stability levels and the necessary control power for the aircraft concept.

The flight mechanics tasks within the conceptual design phase involve sizing and positioning of control surfaces so that a permissible flight mechanics centre of gravity range can be defined. Additionally, the design choices must also cater for the possibility to achieve desirable FQ/HQ whilst meeting manoeuvre and trim design targets. The initial analyses investigate aspects of stability and control, trim capabilities, failure cases and performance. Feedback is provided on the design, or requirements, of the overall sizing of the aircraft.

4.1 Performance Characteristics of Pitch Instability

The mission requirements placed upon an advanced aircraft concept often have contradicting design solutions. For instance, a requirement for high instantaneous turn rate at subsonic speeds demands a large wing area and a high trimmable lift coefficient. A requirement for high supersonic specific excess power (SEP) demands low supersonic drag through a swept low aspect ratio wing, small wetted area and slender configuration. Through the introduction of unstable characteristcs in pitch, it is possible to alleviate such design compromises and help achieve balance between the different requirements. The flight mechanics role is therefore one of defining the performance gain for feasible instability levels within control power constraints considered about all axes.

As an example, Figure 7a illustrates the reduced drag coefficient with aft movement of the CG for a 3g-turn at Mach 0.7. The results are shown relative to the drag coefficient of the reference CG location, $\Delta CG\ \%MAC = 0$. Close to 15% drag reduction for this particular performance point is found for the largest elevon at a CG location equivalent to $10\%MAC$ from the reference CG. Figure 7b shows the reduction in airspeed for 1g level flight for different angles of attack at mean sea level. The results are plotted for different elevon-to-wing chord ratios, c_e/c_w and levels of instability. Increments of $\Delta CG\ \%MAC$ represent an aft movement of the CG.

The performance gains are due to the necessary trailing edge-down deflections required to trim the aircraft in various flight conditions. The effect increases for aft movement of the CG and the trimmed lift coefficients can be used to update the aircraft sizing in the next iteration. Exploiting the full potential of unstable characteristics will however for instance leave insufficient control surface deflection margin for entering and exiting manoeuvres. The reduction in control surface margin is due to control surfaces approaching the limits of the deflection range in order to trim. The level of instability is thus traded against several criteria. Figure 7 shows that larger control surfaces allow further performance gain with aft CG movement.

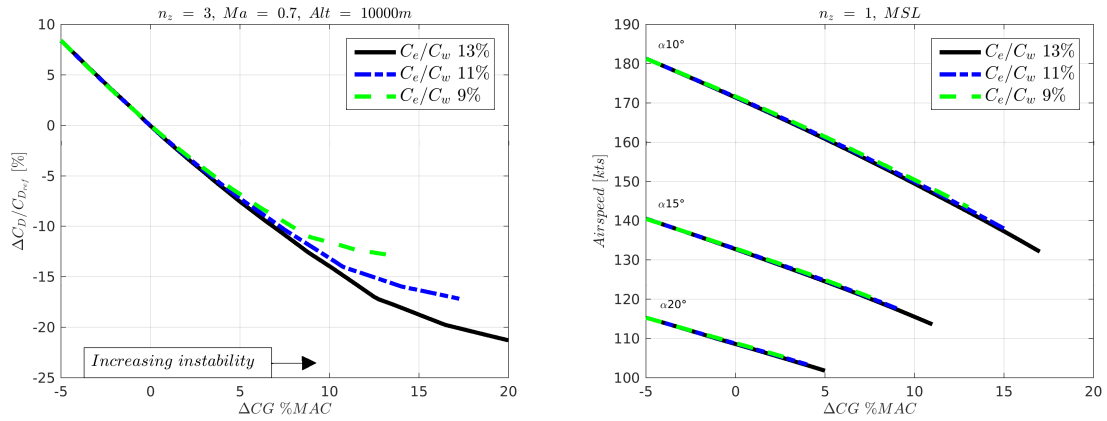

(a) Relative drag coefficient vs aircraft instability (b) Trimmed airspeed vs aircraft instability

Figure 7 – Performance metrics for different CG locations, $\Delta CG\ \%MAC$, and elevon-to-wing chord ratios, c_e/c_w.

Figure 8 shows a constant-radius-loop manoeuvre performed for two levels of longitudinal stability. Prior to the entry of the loop, the throttle is set equal for comparison of the performance between the two cases. The results quantify the decreased angle of attack and the increased elevator deflections necessary for the longitudinally unstable configuration to complete this particular manoeuvre. Additionally, the more unstable configuration exits the manoeuvre with higher kinetic energy as illustrated by difference in travelled distance.

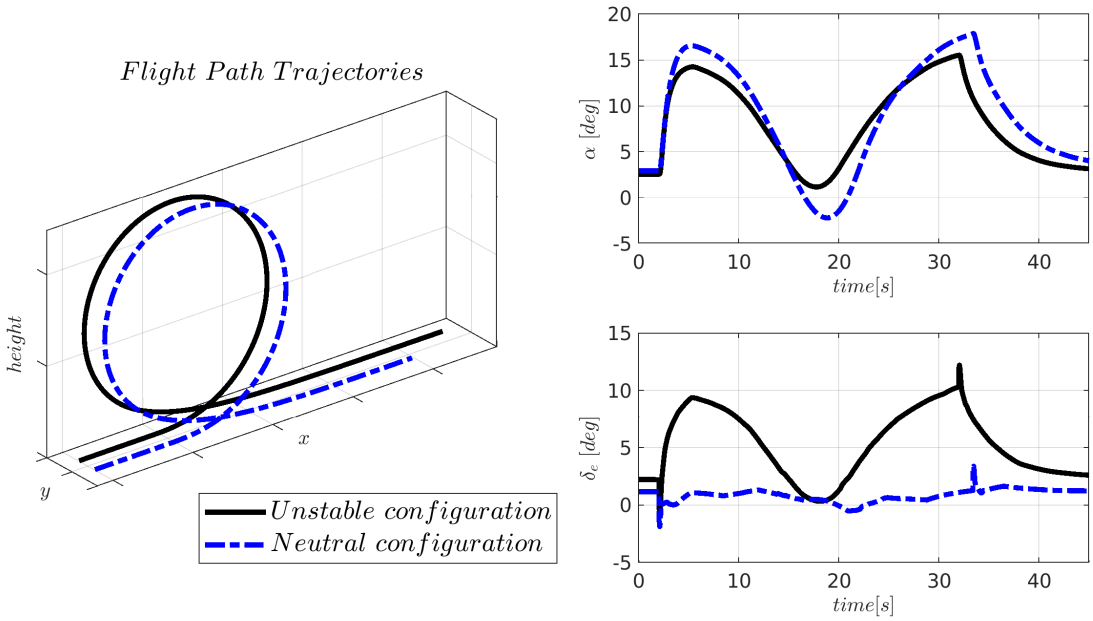

Figure 8 – Constant-radius-loop performed with a longitudinally neutrally stable configuration and an unstable configuration. The maneuvers are offset somewhat in the y-direction for improved legibility

4.2 Pitch Recovery

The sizing of the control surfaces must be evaluated in relation to centre of gravity limits and the boundaries of the permissible flight envelope. For an unstable aircraft configuration, the minimum installed control power as well as the control power build-up rate must be correlated to the control and stability requirements around all axes. For instance, sufficient control power must ensure safe recovery and the ability to perform pitch recovery due to disturbances and rolling at high angles of attack[2].

It is possible to perform open-loop simulation of the unaugmented unstable aircraft to evaluate pure pitch-down capability against some design criteria. With an implemented FCS, additional criteria may be included in the analysis. As an example, for a given required minimum roll acceleration, sizing of the control power can be evaluated whilst taking into account effects of coordinating a coupled pitch-roll input, i.e. maintaining angles of sideslip within boundaries. Additional effects include inertial coupling and the reduced control budget due to differential deflection. The recovery margin should include the reduced control budget for coupled manoeuvres and the inertial moment due to max commanded roll rate at positive and negative angles of attack.

Figure 9 shows the acquired pitch and roll acceleration from a coupled command input from a flight condition close to maximum angle of attack. The results are plotted for different scaling of the control power (ΔCP) and levels of instability. ΔCP 10% corresponds to the baseline control power plus an additional 10%. The manoeuvre is performed against design criteria for the minimum required pitch and roll acceleration. It can be noted that with aft movement of the CG, i.e. increased instability, the acquired roll respone is degraded below the design criterion for roll acceleration. This is partly due to the proritisation of the FCS for allocation of control deflections to the pitch channel. With the configurable control law parameters incorporated into the model, it is possible to tune the response and control allocation in order to evaluate close to max performance of the augmented airframe.

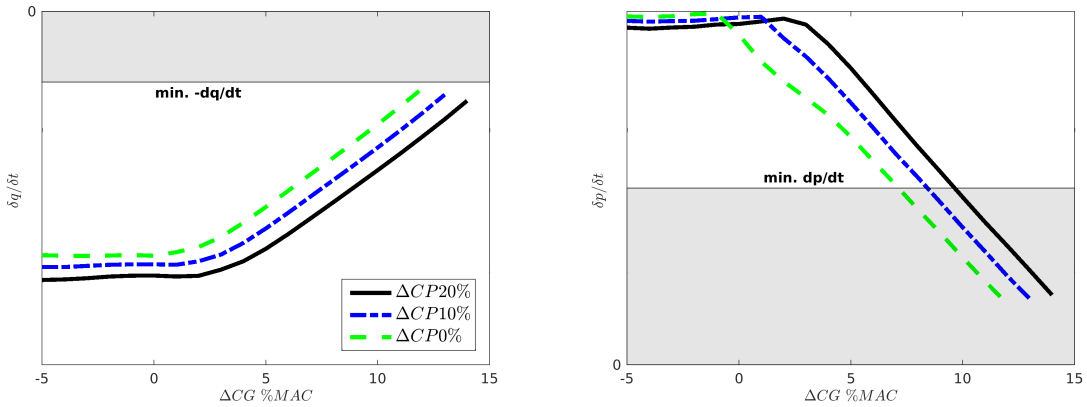

(a) pitch acceleration vs instability

(b) roll acceleration vs instability

Figure 9 – Pitch and roll response from a coupled control input close to α_{max}.

4.3 Take-Off Rotation

One goal is to evaluate the nose wheel lift-off capability using flight dynamics simulation. This is done in relation to the forward centre of gravity limitation, landing gear placement and control surface sizing[3]. The evaluation can be based on a desired rotation speed or take-off distance, where the latter requires suitable engine modelling. Additionally, the required nose wheel lift-off speed should be below the minimum flying speed so that the take-off performance is not limited by the capability to rotate.

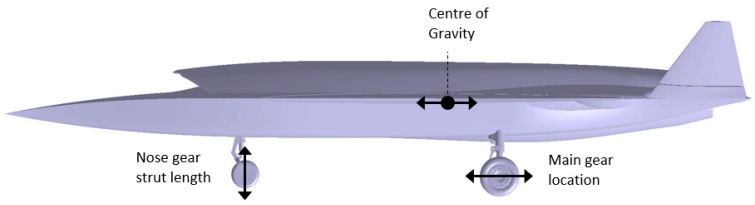

Figure 10 – Saab FCAS sideview. Flight mechanics landing gear design parameters

The design trade also includes the nose gear strut length as a design parameter in order to vary the installed angle of attack, or angle of incidence, of the aircaft as shown in Figure 10. The installed angle of attack, α_{inst}, is mainly varied by setting the nose-gear strut length but also depends on the compression of the landing gear. The landing gear compression, in the model, is a function of centre of gravity location, a/c mass, main landing gear placement and the landing gear spring stiffness. Limitations are also included with regards to:

- Max allowable tip back angle
- Landing gear load distribution

Open-loop simulations were conducted by applying a full nose-up command and finding the speed for zero compression force on the nose gear strut, i.e. the minimum nose wheel lift-off speed. Effects captured in the simulations include the thrust vector alignment, strut forces (compression, damping) and aerodynamic force corrections among others.

In Figure 11, results are plotted for varying control power and CG location. The two sets of curves with regards to the control power correspond to different installed angles of attack(AoA), where $\alpha_{\text{inst,ref}}$ is the reference installed AoA. The impact of increasing the $\alpha_{\text{inst,ref}}$ by three degress is highlighted with regards to the rotation capability versus CG location. The CG location for the same nose wheel lift-off speed is shifted forward several units of $\%MAC$. At a certain point, with aft movement of the CG, the distance between the CG position and the main-gear position will be limited by the tip back angle requirement as illustrated by the red lines.

High level commands to perform closed-loop simulation of the entire take-off phase have been used to study the field performance requirements. For these simulations the FCS is fed with a commanded pitch angle to establish the climb-out and overall take-off performance is studied.

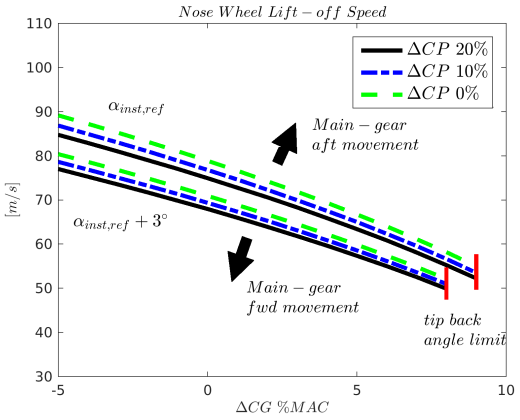

Figure 11 – Rotation capability in terms of minimum speec for nose wheel lift of as a function of CG location and control power.

In case the stability and control requirements, due to the performance requirements, dictate the aft-most centre of gravity location, the main landing gear will have to be placed accordingly, so that the requirements for tip back angle and load distribution are satisfied. Therefore, there is a coupling with the forward centre of gravity location given a certain requirement on the lift-off speed. Aft movement of the main landing gear will have a similar effect as decreasing the $\alpha_{\text{inst,ref}}$, which is indicated by the arrows in Figure 11. This is due to that the distane between the CG and main landing gear increases. Hence, the forward centre of gravity location will have to be shifted aftwards to satisfy the given lift-off speed requirement.

4.4 Control Surface Failure

Risks and limitations caused by failure of a primary actuators are important to consider in the conceptual stage. Servo or actuator failure modes can have a large influence on the ability to perform safe flight and should be considered in the control surface sizing and allocation process. Certain actuation techniques cannot be designed with sufficiently low failure probabilities and fault tolerance to meet necessary safety levels for an aircraft.

The goal is to, early on in the conceptual stage, study the influence of the different servo failure modes. With the flight mechanics and FCS model, the influence of servo failures can be studied in a number of ways. The trimmable envelope can be investigated for different control strategies as well as dynamic flight phases in which the aircraft is manoeuvred back to landing with a failed control surface. Depending on the type of failure exprienced as well as the configuration of the aircraft, different parts of the envelope will be affected.

There are two failure cases to be considered. Jamming is the first, which means that the actuator is

locked in a certain position. The second case is floating, in which the control surface deflection varies dynamically with the flight condition. Free and damped floating cases are primarily considered for hydraulic actuators whereas jamming should be considered for electromechanical actuators as well.

Figure 12 illustrates the trimmable envelope with one of the outer control surfaces jammed at 10 degrees trailing edge-down deflection. The results in Figure 12a are for the baseline control surface configuration comprising two elevons on each wing. The coloured areas represent the trimmable envelope of the aircraft for the given CG location and contol surface size. The numbering on the contours shows the required deflections of the inner elevon to compensate for the jammed elevon. The transonic region poses a particular problem with significant variation in the stability of the aircraft. Figure 12b shows the restored trimmable envelope for the specfic CG location after resizing of the control surfaces. The resizing was done by splitting the trailing edge flap into three elevons, similar to the example in Figure 3.

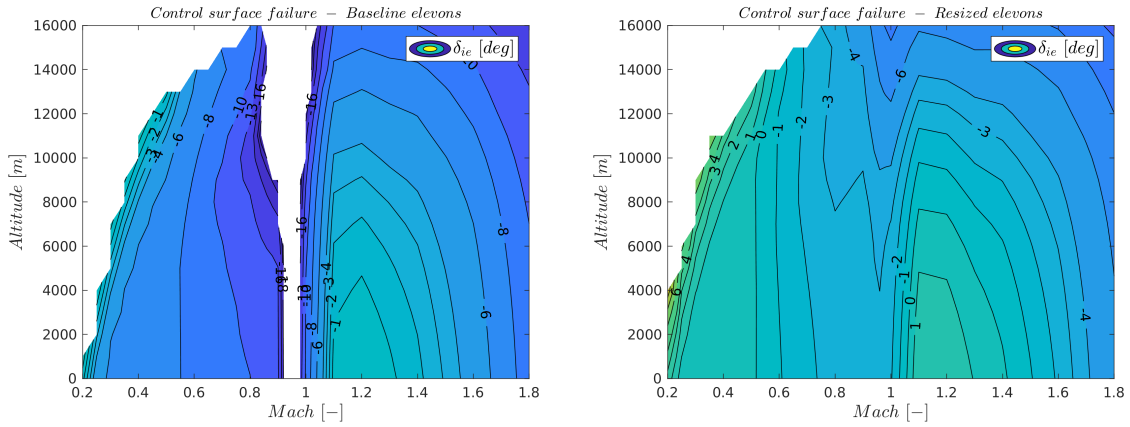

(a) Baseline elevon geomtery

(b) Resized elevon geomtery

Figure 12 – Outer elevon jamming failure. Inner elevon deflections, δ_{ie}, within the trimmable envelope before and after resizing of the elevons.

Figure 13 shows a case in which a servo failure is suffered during a turning manoeuvre. The left outer control surface (δ_{LOE}) is locked in its position at a large deflection. The red cross indicates, in space and time, the occurence of the failure event. After a specified time delay, the FCS will notice the fault and reconfigure the control allocation to be able to control the aircraft and continue flying. Metrics for control surface activity and deviations from the ideal flight path can be employed to evaluate the degradation of the handling qualities due to failure modes[4].

The bottom plots in Figure 13 show the deflections for each control surface. There is an increased control surface acitivity for the inner control surfaces, δ_{LIE} and δ_{RIE}, following the failure event. The roll acceleration, $\delta p/\delta t$, is reduced, i.e. the responsiveness in roll is degraded, by roughly 50%. However, the aircraft is still able to achieve close to the same roll rate performance and follow the flight trajectory without signficant deviations compared to the nominal case.

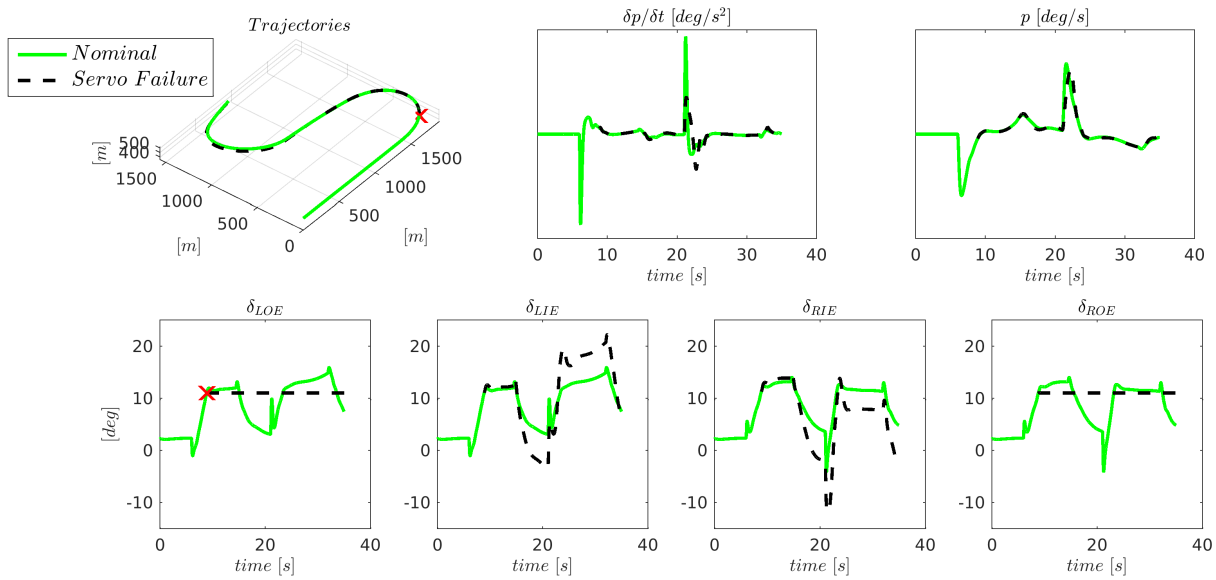

Figure 13 – Closed-loop simulation with servo failure.

4.5 Dynamic Manoeuvres and Subsystem Sizing

One example where closed-loop simulations are used is when studying trade-offs between the requirements for performance and actuator capacity for various configurations. It is necessary to have acceptable levels of hinge moment throughout the flight envelope. Excessive instability will require large trimmed deflections in the subsonic regime as well as high actuation rates and hinge moments. This will increase the demand on the various related subsystems with regards to cooling, power supply, actuator capacity, packaging among others.

Static analysis can be used to investigate the trimmed hinge moments which can readily be altered by varying the stability and control of the aircraft for steady flight conditions. The transient hinge moments required to enter and exit demanding manoeuvres can still vary significantly. A 6-DOF model with implemented control laws that provide control scheduling for different modes and monitoring of limits can be used to control instantaneous and steady manoeuvres. Together with outer loop functions to perform various operational manoeuvres, it is possible to conduct a much more comprehensive analysis. Capturing transient hinge moments as well as the combinations of hinge moments and control surface deflection rates improves the design feedback and can enable more accurate requirements specifcation of hardware systems to be determined earlier in the conceptual phase.

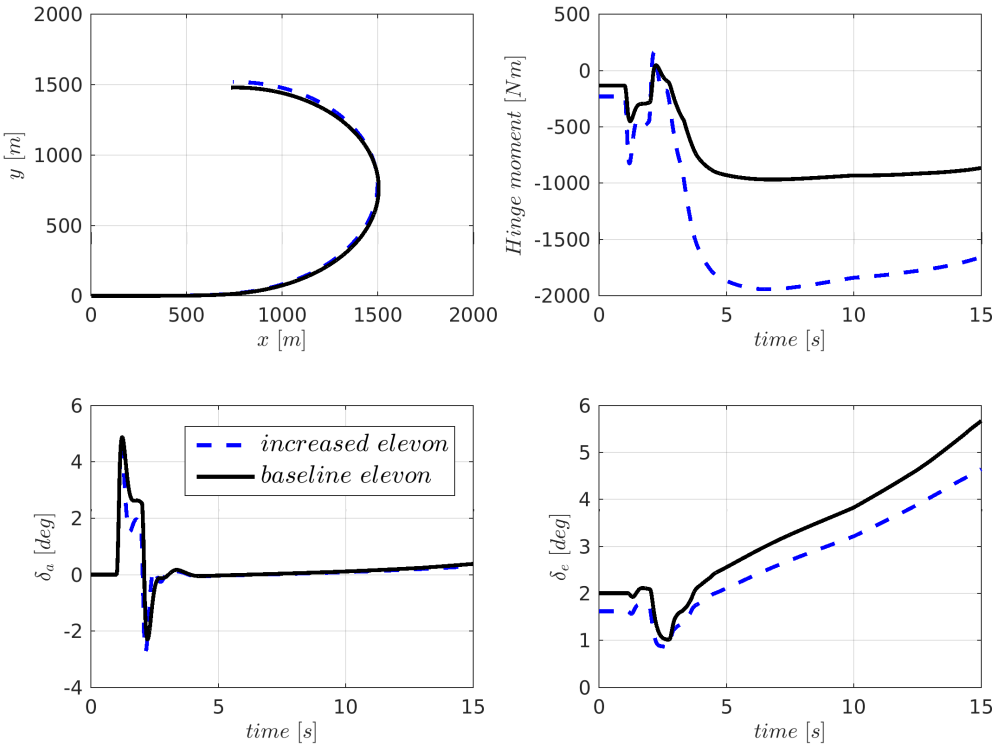

Figure 14 – Wind-up turn using two different elevon sizes. Trajectories (top left), Elevon hinge moments (top right), roll deflections, δ_a (bottom left), pitch deflections, δ_e (bottom right).

Figure 14 shows a constant load factor turn using two different elevon sizes. The results show the difference in hinge moment and control margin to perform the manoeuvre. The bottom left figure illustrates, for the baseline elevon, the additional roll deflection, δ_a, required to establish the commanded roll rate and necessary bank angle. The bottom right shows the increment in pitch deflection, δ_e, to maintain the constant load factor throughout the turn. Although the deflections are smaller for the larger elevon, the hinge moment is increased. Turbulence modelling can also be included to account for the demands of stabilization. Such data is then provided to initiate sizing of subsystems like the actuation system.

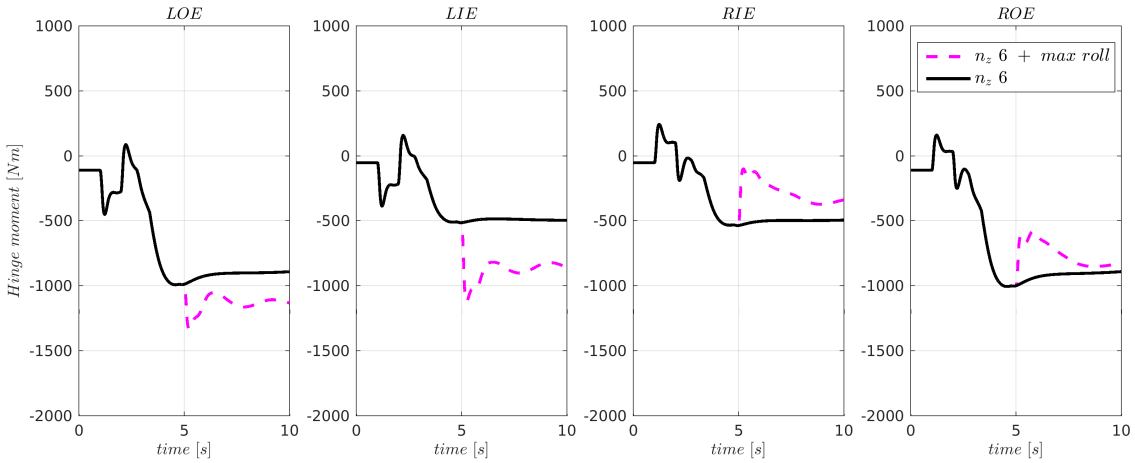

Figure 15 – Hinge moments during two manoeuvres. Wind-up turn (black), wind-up turn + roll from a loaded flight condition(purple).

Depending on the type of manoeuvre used for sizing, the magnitude of the dynamic hinge moment can vary substantially. In Figure 15, the hinge moment for all four elevons is plotted in the order: left outer elevon(LOE), left inner elevon(LIE), right inner elevon(RIE) and right outer elevon(ROE). The time histories show the hinge moments for two different manoeuvres. In the first, a wind-up turn is performed with a load factor of 6g and in the second, the same manoeuvre is performed with the addition of a max roll input when the load factor has built up at around 5 seconds. It is shown that the resulting hinge moment is significantly increased for the elevons on the left wing. The transient spike in the hinge moment is due to the additional deflections required to achieve the roll response set by the FCS from a loaded flight condition. In order to limit the impact of the more aggressive manoeuvring on the demands, configurable parameters in the control laws can be tweaked which alter the response of the aircraft whilst still commanding the same roll rate. Hence, it is possible to show trade-offs such as actuation power and cooling demands for various configurations and performance requirements.

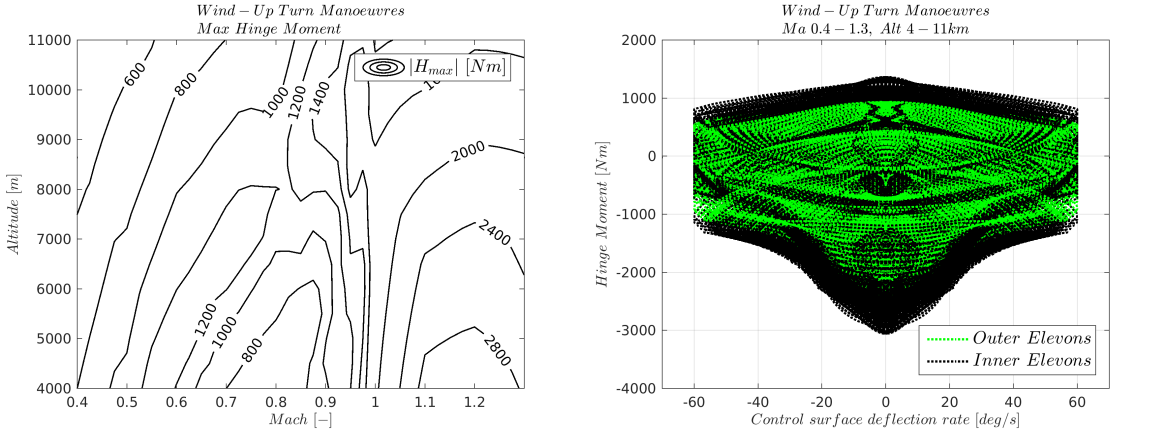

(a) Max hinge moment experienced by any control surface

(b) Distribution of hinge moments and control surface rates between outer and inner elevons

Figure 16 – Results from dynamic manoeuvres performed throughout the flight envelope

From Figure 15 it is possible to find the maximum hinge moment experienced during one manoeuvre at a certain point within the flight envelope. It is of interest to study the maximum achieved hinge moments as well as the combination of control surface rates and moments within several parts of the envelope. Figure 16a shows the absolute maximum hinge moment, $|H_{max}|$, attained by any control surface during wind-up turns, with a target load factor of 6 for subsonic flight conditions and a target load factor of 3 for supersonic, at various points within the flight envelope. It can be noted that for the subsonic regime, the maximum hinge moments are experienced around a constant dynamic pressure line corresponding to Mach 0.55 at an altitude of 4000 m.

All the combinations of hinge moments and control surface rates achieved whilst performing the wind-up turn manoeuvres throughout the flight envelope are mapped out in Figure 16b. The maximum control surface rate is set by the FCS and can be varied for the analysis. High control surface rates in combination with high hinge moments will increase the requirements of the actuator capacity, which in turn will increase the necessary power supply, cooling, structure, size and weight of various subsystems. It is possible to note that the outer elevons are overall subjected to smaller hinge moments compared to the inner elevons. The difference can be adjusted by, for instance, changing the control allocation or resizing the control surfaces. The response characteristcs can be altered to reduce areas in Figure 16b where high power supply is required, i.e. when high rates are demanded in combination with high hinge moments. Additionally, varying the CG location will shift the results up or down depending of the level of instability.

5. Conclusions

The use of flight dynamics simulation and FCS auto-generation in the conceptual design phase has greatly increased the efficiency of the design of the unstable supersonic aircraft described in this paper. Results from the flight mechanical simulation has provided early design feedback and validation of the initial aircraft sizing in relation to applicable requirements.

The flexible framework allowing for variation of key parameters has allowed for a better quantification of costs and benefits of various design trades in terms of, for exampe, the desired center of gravity. Examples from the conceptual design of a supersonic fighter has quantified possible drag benefits and maneuvre limitations stemming from a more aft center of gravity placement. Examples have also highlighted a trade-off from control surface sizing in terms of manoeuvre capability and control surface hinge moments.

A more representative connection between mission requirements and subsystem sizing of the actuation system has been facilitated by the possibility of simulating relevant mission maneuvers. The connection can be utilised for both precise requirement specifications of the actuation system and for assessment of the mission capabilities with a certain design choice.

6. Contact Author Email Address

mailto: emil.johansson@saabgroup.com

7. Copyright Statement

References

[1] Verhagen W, Bermell-Garcia P,van Dijk R and Curran R. A critical review of Knowledge-Based Engineering: An identification of research challenges. *Advanced Engineering Informatics*, Vol 26, Issue 1, January 2012, pages 5-15.

[2] Mangold P. Integration of Handling Quality Aspects into the Aerodynamic Design of Modern Unstable Fighters. *AGARD-CP-508*, Friedrichshafen, 1990.

[3] Kaminer I, Howard R and Buttrill C. Development of Closed-Loop Tail-Sizing Criteria for a High Speed Civil Transport. *Journal of Aircraft*, Vol. 34, No. 5, September-October 1997.

[4] Callaghan P and Kunz D. Evaluation of Unmanned Aircraft Flying/Handling Qualities Using a Stitched Learjet Model. *Journal of Guidance,Control, and Dynamics*, Vol. 44, No. 4, April 2021.